

Incorporation of Mg^{2+} , Sr^{2+} , Ba^{2+} and Zn^{2+} into aragonite and comparison with calcite

M. Menadakis · G. Maroulis · P. G. Koutsoukos

Received: 28 September 2008 / Accepted: 30 September 2008 / Published online: 7 November 2008
© Springer Science+Business Media, LLC 2008

Abstract We have investigated the presence of foreign ions into the bulk structure and the external surfaces of aragonite using periodic ab-initio methods. Four cations isovalent to Ca^{2+} were studied: Mg^{2+} , Sr^{2+} , Ba^{2+} and Zn^{2+} . The calculations were performed at structures (bulk, surface) that contain four and eight CaCO_3 units. Our results, at the Hartree-Fock level, show that the incorporation of those ions into aragonite depends strongly on their size. Mg^{2+} and Zn^{2+} , due to their smaller size, can substitute Ca^{2+} ions in the crystal lattice while the incorporation of Sr^{2+} and Ba^{2+} into aragonite is energetically less favoured. Examination of the [011], [110] and [001] surfaces of aragonite revealed that the surface incorporation reduces the energetic cost for the larger ions. These systems provide challenging examples for most shape analysis methods applied in Mathematical Chemistry.

Keywords Aragonite · Calcite · Crystal impurities

1 Introduction

Calcium carbonate is the most common of all carbonate minerals. It is known to exist abundantly in natural systems and has three polymorphic forms: calcite, aragonite and vaterite. The first two are abundant in geological and biological systems while the third one is the least stable form in ambient conditions. Besides these anhydrous forms,

M. Menadakis · G. Maroulis (✉)
Department of Chemistry, University of Patras, 26500 Patras, Greece
e-mail: maroulis@upatras.gr

P. G. Koutsoukos (✉)
Department of Chemical Engineering, University of Patras and FORTH-ICEHT,
P.O. Box 1414, 26504 Patras, Greece
e-mail: pgk@chemeng.upatras.gr

calcium carbonate can also exist as two hydrated forms namely monohydrocalcite and calcium carbonate hexahydrate.

Calcium carbonate can be used as filler in asphalt, paints, papers, plastics and rubber, as a fixed controller in the manufacture of steel, iron and so forth [1]. These industrial applications require an accurate control of the crystallization of calcium carbonate. This control may be achieved by structured organic surface templates such as self assembled monolayers [2,3], biomacromolecules and functionalized polymers [4]. Morphology variations and polymorph selectivity can be also obtained by growth in solution in the presence of growth modifiers such as ions [5], natural and synthetic polymers [6–8].

All these processes involve interactions between the crystal structure (bulk or surface) with foreign ions, molecules and polymers [9–11]. In order to understand the factors that control crystal growth, dissolution and reactivity there must exist an accurate description of the crystal structure in an atomic scale. The physico-chemical properties of calcium carbonate have been the object of numerous theoretical and computer simulation studies [12–17]. These studies include surface-water interactions [18], adsorption of molecules on surfaces [12,13], elastic constants [14], electrical and optical properties [15–17].

Although calcite is the thermodynamically most stable polymorph, various polymorphs and morphologies of calcium carbonate are formed depending on the experimental conditions [19]. Of importance to the growth of calcium carbonate polymorphs in the presence of metal ions is their interaction with the growing phase. For instance, the trace element content of the calcium carbonates has often been used as a guide to understand rock paragenesis [20]. One frequently suggested mechanism for controlling calcium carbonate polymorph formation involves the introduction of a specific inhibitor of calcite which favours the aragonite polymorph [21]. It is interesting to note that Aragonite is formed predominantly in living organisms and in Mg- and Sr-containing solutions [22]. Magnesium is known to induce aragonite formation from sea water, and *in vitro* at ratios of $Mg/Ca > 4$. Polymorphic phases of calcium carbonate, stable at high pressures, do depend on the incorporation of divalent ions in the lattice [23].

The incorporation of trace metal ions in biogenic carbonates provides information the chemistry of both historic and modern oceanic seawater. Historic information about climate change [24], oceanic nutrient geochemistry [25], deep-ocean circulation patterns [26,27], histories of anthropogenic metal pollution [28,29] and reconstructed patterns in El Nino Southern Oscillations [30,31] can all be elucidated from carbonate-bound trace metals. The partition of metal ions in calcium carbonate polymorphs may be detrimental to the stability of metastable phases. Trace metals (Sr, Ba), in otolith aragonite have been determined in fish bone [32].

Motivated by the importance of these observations, in this paper we examine the way of incorporation of magnesium ions into bulk and some low index surfaces of aragonite. Along with Mg^{2+} , three other isovalent to Ca^{2+} ions were studied (Sr^{2+} , Ba^{2+} and Zn^{2+}) regarding their ability to substitute the calcium ions. These results can be compared with our previous work on calcite [33] to assess the effect on the structural and energetic characteristics of the incorporation on the two most stable phases of calcium carbonate.

2 Computational details

The CRYSTAL98 [34] program permits the calculation of the wavefunction and properties of crystalline materials within the Hartree-Fock Linear-Combination-of-Atomic-Orbitals (HF-LCAO). We have utilised Gaussian basis functions for the quantum chemical description of the calcium, carbon and oxygen centers present in the unit cell of aragonite. The corresponding basis sets have been previously tested in calcite and other crystalline compounds with the outer d orbitals for each atom reoptimized in the environment of aragonite with respect to the total energy. Calcium carbonate in the form of aragonite crystallizes in the orthorhombic crystal system with four calcium carbonate units in the unit cell (Fig. 1).

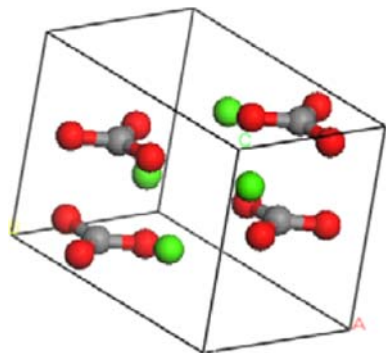
Building structures (bulk or surface) with multiple calcium carbonate units, using the supercell approach, and subsequent substitution of the calcium cations could provide an estimate of the effect of the degree of contamination in the defect formation energy. The substitutional defect formation energy is given by

$$\Delta E_X = E_{\text{CaCO}_3-X} - N E_{\text{CaCO}_3} + E_{\text{Ca}^{2+}} - E_{X^{2+}} \quad (1)$$

where E_{CaCO_3-X} ($X = \text{Mg}^{2+}, \text{Sr}^{2+}, \text{Ba}^{2+}$ and Zn^{2+}) is the total energy of the defective structure, N is the number of the calcium carbonate units in the corresponding perfect lattice supercell, E_{CaCO_3} is the bulk energy per formula unit of aragonite and $E_{\text{Ca}^{2+}}$, $E_{X^{2+}}$ are the total energies of the isolated ions. The construction of the surfaces of aragonite was based on the slab model (two sided crystal faces). The surfaces that we have examined are (011), (110) and (001). The last one is of special interest because it can be terminated either by calcium cations or carbonate groups as shown in Fig. 2.

The incorporation of Mg^{2+} ion into bulk aragonite was further analysed by relaxing the environment around the defect. Mg^{2+} is surrounded by nine O atoms that are organized in four groups. The first neighbour of the Mg^{2+} defect consist of one oxygen atom and the relaxation was performed by changing its cartesian coordinates. The defect formation energy was calculated both on the relaxed and unrelaxed structure yielding the response of the bulk structure to the formation of the defect.

Fig. 1 The unit cell of aragonite



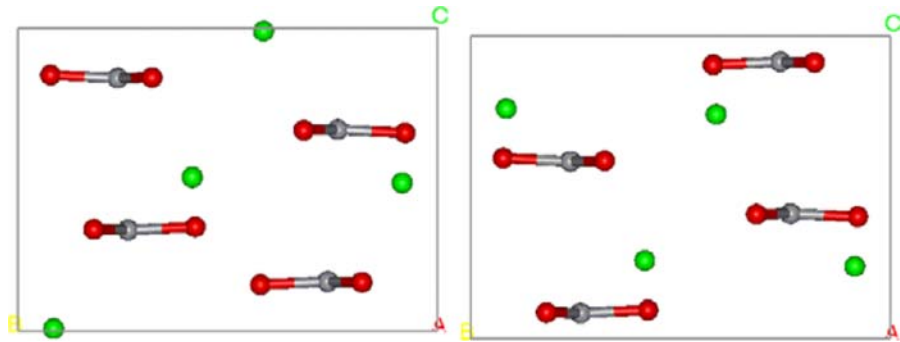


Fig. 2 Unit cell of [001] surface of aragonite terminated by calcium ions (left) or carbonate groups (right)

3 Results

Table 1 shows the defect formation energy for the incorporation of Mg^{2+} , Sr^{2+} , Ba^{2+} and Zn^{2+} ions into aragonite bulk structure. The calculations were performed at two different cells (bulk or surface) with four and eight structural units. The degree of contamination ranged from 13 up to 100% meaning that all the Ca^{2+} are substituted with the foreign ions. A negative value of the defect formation energy indicates that the incorporation is energetically favoured while its absolute value measures the ability of the foreign ions for the incorporation. In bulk aragonite, ions that are smaller than Ca^{2+} (Mg^{2+} , Zn^{2+}) can enter the host lattice substituting calcium ions while the incorporation of Sr^{2+} and Ba^{2+} is less favoured at the studied degrees of contamination. The size of the foreign ion is probably the most important factor that controls

Table 1 Defect formation energy [eV] of X^{2+} ($\text{X}=\text{Mg}$, Sr , Ba , Zn) doped aragonite

%	Mg^{2+}	Sr^{2+}	Ba^{2+}	Zn^{2+}
4 CaCO_3 units				
25	-2.2580	1.8559	5.4579	-2.5317
50	-4.5082	3.7141	10.9123	-5.0503
75	-6.7465	5.5854	16.4033	-7.5587
100	-8.9772	7.4594	21.8911	-10.0537
8 CaCO_3 units				
13	-2.2601	1.8550	5.4517	-2.5351
25	-4.5162	3.7117	10.9155	-5.0633
38	-6.7682	5.5691	16.3640	-7.5864
50	-9.0164	7.4283	21.8248	-10.1014
63	-11.2569	9.2988	27.3104	-12.6148
75	-13.4931	11.1710	32.8062	-15.1177
88	-15.7258	13.0441	38.2893	-17.6188
100	-17.9544	14.9189	43.7823	-20.1088

the procedure of incorporation. Figure 3 shows the electron density maps of Zn^{2+} and Sr^{2+} doped aragonite where Sr^{2+} due to its larger size induces larger distortion to the crystalline lattice contrary to Zn^{2+} whose size approaches the size of calcium cation.

The incorporation of Mg^{2+} , Sr^{2+} , Ba^{2+} , and Zn^{2+} into the bulk structure of aragonite and calcite is summarized in Fig. 4. The general trend of incorporation does not change but the energetic content of the substitution of calcium ions varies from aragonite to calcite. The defect formation energy, ΔE_X , is shifted towards higher energy values for the smaller ions while the opposite stands for the larger ions like Sr^{2+} and Ba^{2+} .

The relaxation procedure was performed only for the incorporation of magnesium cation due to the high computational cost. The results are presented in Table 2 where comparison is made with the analogous results for the incorporation of Mg^{2+} into calcite bulk structure. In the relaxed structure of the Mg^{2+} doped aragonite there is an energy gain of approximately 0.06 eV while the first neighbouring oxygen atom

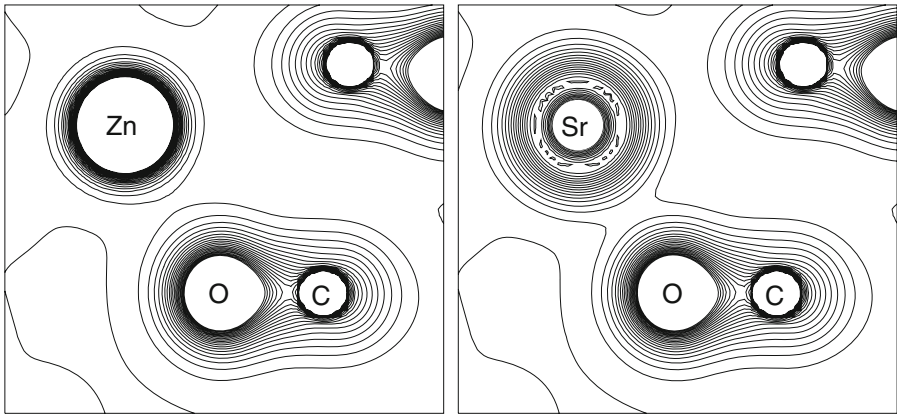


Fig. 3 Electron density maps of Zn^{2+} (left) and Sr^{2+} (right) doped aragonite

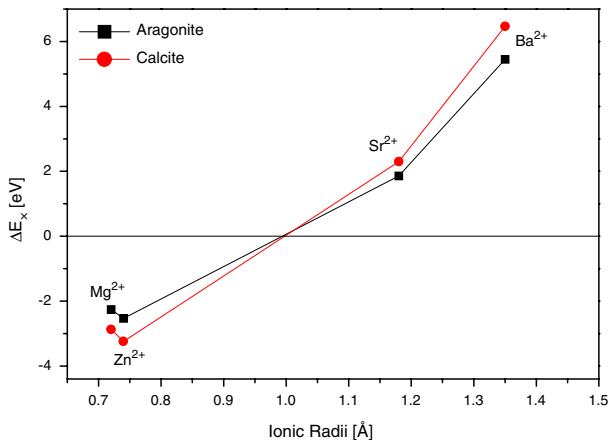


Fig. 4 Incorporation of Mg^{2+} , Sr^{2+} , Ba^{2+} , and Zn^{2+} into aragonite and calcite

Table 2 Defect formation energy [eV] of Mg^{2+} doped aragonite and calcite in the unrelaxed and relaxed structures. ΔR is the difference in Mg–O distance upon relaxation

	Aragonite	Calcite	
	25%	50%	25%
Unrelaxed	–2.2580	–2.8744	–2.8740
Relaxed	–2.3102	–3.3507	–3.4278
Mg–O [Å]	2.3262	2.2467	2.2457
ΔR [Å]	–0.0895	–0.1252	–0.1262

Table 3 Defect formation energy [eV] of X^{2+} ($X=Mg, Sr, Ba, Zn$) doped surfaces of aragonite

Surface	13%			
	Mg^{2+}	Sr^{2+}	Ba^{2+}	Zn^{2+}
[011]	–1.8638	1.3592	3.8603	–2.3149
[110]	–1.8028	1.2648	3.5223	–2.2979
[001]Ca	–1.4458	0.7987	2.0260	–2.3016
[001]CO ₃	–1.8409	1.3490	3.8500	–2.2718

exhibits an inwards relaxation (the Mg–O distance decreases). In calcite the energy gain due to the relaxation is approximately ten times larger when compared to aragonite. This is probably due to different symmetry of the two crystalline lattices because the relaxation in calcite involves the displacement all (six) oxygen atoms while in aragonite only the closest, to Mg^{2+} cation, oxygen atom is moved from its equilibrium position.

The energetic content of the incorporation of Mg^{2+} , Sr^{2+} , Ba^{2+} and Zn^{2+} on the surfaces of aragonite is summarized in Table 3. The negative sign of the defect formation energy for Mg^{2+} and Zn^{2+} indicates that the incorporation of these cations is energetically favoured in all surfaces. Comparing ΔE_X it emerges that Zn^{2+} can be incorporated in the surfaces of aragonite more easily than Mg^{2+} . The incorporation of Sr and Ba follows the trend that appeared in bulk structure as the defect formation energy is 1.3 and 3.8 eV, respectively for the substitution of the first calcium cation. Table 3 shows that the incorporation all cations differentiates in the [001] Ca surface of aragonite. The defect formation energy is decreasing by absolute value for Mg^{2+} , Sr^{2+} , and Ba^{2+} with the largest difference (>1.5 eV) being observed in the incorporation of Ba^{2+} .

Comparison of the incorporation of Mg^{2+} , Sr^{2+} , Ba^{2+} and Zn^{2+} into bulk and surfaces of aragonite is made in Fig. 5. In all cases there is a clear difference in the incorporation in [001] as the terminal group of the surface influence strongly the energetic content of the incorporation. The incorporation of Mg^{2+} and Zn^{2+} is more favoured when the [001] is terminated with calcium cations while for the larger ions (Sr^{2+} and Ba^{2+}) the incorporation in (001) CO₃ reduces the energetic cost. Mg and Zn prefer to be incorporated in the bulk structure of aragonite as the defect formation energy is about 0.5 and 0.25 eV lower, respectively. The opposite stands for Sr and Ba

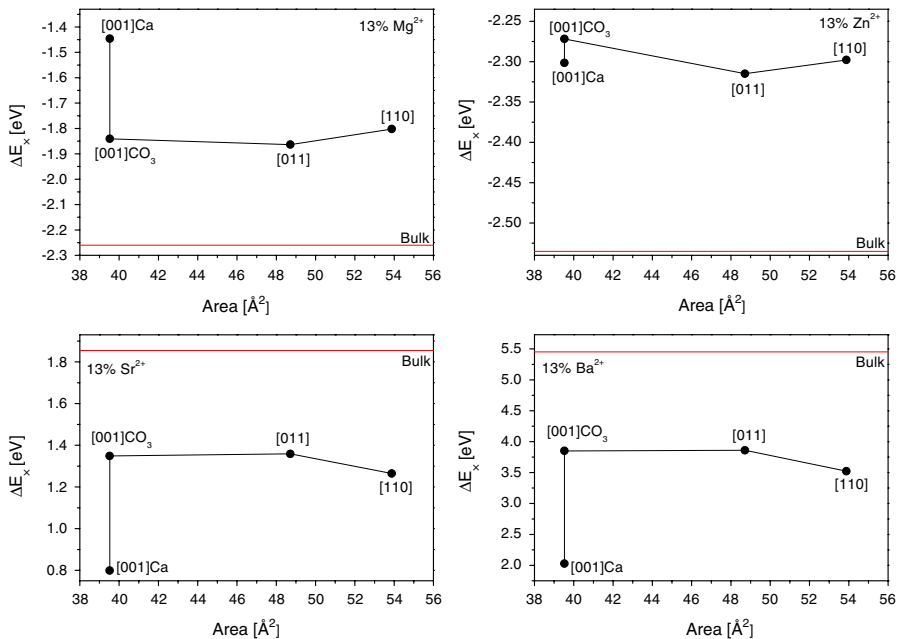


Fig. 5 Incorporation of Mg^{2+} , Zn^{2+} , Sr^{2+} and Ba^{2+} into bulk and surfaces of aragonite

meaning that the free space above the surfaces of aragonite makes less difficult the substitution of calcium cations. Nevertheless the sign of the defect formation energy remains positive indicating that the incorporation of these cations is not energetically favoured at degrees of contamination above 13% neither in bulk nor in surfaces.

Acknowledgments M. Menadakis gratefully acknowledges a scholarship from the Institute of Chemical Engineering and High Temperature Chemical Processes of the Foundation of Research and Technology-Hellas (FORTH/ICE-HT).

References

1. J.C. Cowan, D.J. Weintritt, *Water Formed Scale Deposits* (Gulf, Houston, TX, 1976), p. 112
2. J. Aizemberg, A.J. Black, G. Whitesides, *Nature* **398**, 495 (1999)
3. Y.J. Han, J. Aizemberg, *J. Am. Chem. Soc.* **125**, 4032 (2003)
4. R. Lakshminarayanan, S. Valiyaveetil, G. Luan Loy, *Cryst. Growth Des.* **3**, 953 (2003)
5. Y. Zhang, R.A. Dawe, *Chem. Geol.* **163**, 129 (2000)
6. S.M. D'Souza, C. Alexander, S.W. Carr, A.M. Waller, M.J. Whithcombe, E.N. Vulfon, *Nature* **23**, 513 (1999)
7. E. Dalas, P. Klepetsanis, P.G. Koutsoukos, *Langmuir* **15**, 8322 (1999)
8. D. Rautaray, A. Sanyal, A. Bharde, A. Ahmad, M. Sastry, *Cryst. Growth Des.* **5**, 399 (2005)
9. J.R. Clarkson, T.J. Price, C.J. Adams, *J. Chem. Soc. Faraday Trans.* **88**, 243 (1992)
10. V. N-Laslo, L. Brecevic, *J. Chem. Soc. Faraday Trans.* **94**, 2005 (1998)
11. Y. Fujita, G.D. Redden, J.C. Ingram, M.M. Cortez, F.G. Ferris, R.W. Smith, *Geochimica et Cosmochimica Acta* **68**, 3261 (2004)
12. S. Hwang, M. Blanco, W.A. Goddard III, *J. Phys. Chem. B* **105**, 10746 (2001)

13. M.A. Nygren, D.H. Gay, C. Richard, A. Catlow, M.P. Wilson, A.L. Rohl, J. Chem. Soc. Faraday Trans. **94**, 3685 (1998)
14. M. Catti, A. Pavese, E. Apra, C. Roetti, Phys. Chem. Miner. **20**, 104 (1993)
15. H.J. Weber, Acta Crystallogr. A **44**, 320 (1988)
16. A.L. Rohl, K. Wright, J.D. Gale, Am. Mineral. **88**, 921 (2003)
17. D. Pohl, R. Rath, Acta Crystallogr. A **35**, 694 (1979)
18. N.H. de Leeuw, S.C. Parker, J. Phys. Chem. B **102**, 2914 (1998)
19. T. Sabbides, E.K. Giannimaras, P.G. Koutsoukos, Environ. Technol. **13**, 73 (1992)
20. J.D. Rimstidt, A. Balog, J. Webb, Geochim. Cosmochim. Acta **62**, 1851 (1998)
21. R. Giles, S. Manne, S. Mann, D.E. Morse, G.D. Stucky, P.K. Hansma, Biol. Bull. **188**, 8 (1995)
22. G.H. Nancollas, M.M. Sawada, J. Petroleum Techn. **34**, 76 (1982)
23. J. Santillan, Q. Williams, Phys. Earth Planet. In. **143–144**, 291 (2004)
24. D.W. Lea, D.K. Pak, H.J. Spero, Science **289**, 1719 (2000)
25. D.W. Lea, G.T. Shen, E.A. Boyle, Nature **340**, 373 (1989)
26. J.F. Adkins, H. Cheng, E.A. Boyle, E.R.M. Druffel, R.L. Edwards, Science **280**, 725 (1998)
27. E.A. Boyle, Science **249**, 863 (1990)
28. G. Schettler, N.J.G. Pearce, Hydrobiologia **317**, 1 (1996)
29. G.D. Price, N.J.G. Pearce, Mar. Poll. Bull. **34**, 1025 (1997)
30. G.T. Shen, C.L. Sanford (1990) in *Global Ecological Consequences of the 1982-83 ElNino-Southern Oscillation*, ed. by P.W. Glynn (Elsevier, 4097 Barium and strontium in protoconch and statolith), p. 255
31. A.W. Tudhope, C.P. Chilcott, M.T. McCulloch, E.R. Cook, J. Chappell, R. Ellam, D.W. Lea, J.M. Lough, G.B. Shimmield, Science **291**, 1511 (2001)
32. B.K. Wells, G.E. Bath, S.E. Thorrold, C.M. Jones Can. J. Fish. Aquat. Sci. **57**, 2122 (2000)
33. M. Menadakis, G. Maroulis, P.G. Koutsoukos, Comput. Mater. Sci. **38**, 522 (2007)
34. V.R. Saunders, R. Dovesi, C. Roetti, M. Causa, N.M. Harrison, R. Orlando, C.M. Zicovich-Wilson, *CRYSTAL98 User's Manual* (Universita di Torino, Torino, 1999)